

# Basis Vector Quantification of Flutter Analysis Structural Modes

Jay S. Northington\*

*TYBRIN Corporation, Eglin Air Force Base, Florida 32542-6865*

DOI: 10.2514/1.42591

A method to concisely quantify, compare, and identify mode shapes for flutter analysis using orthogonalized basis vectors is developed. The procedure numerically describes wing structural mode shapes as scalar projections onto a reduced set of basis vectors. The basis vectors are baseline wing shapes derived from the mode shapes of a reference wing model, and mode shapes from other wing models are concisely related to the basis vectors using the scalar projections. The resulting quantifier describes the wing modes in terms of the physical wing shapes from the reference model. The technique is demonstrated on a simple wing model from which the basis vectors are derived. Mass elements are added to the wing in four different configurations to produce various mode shapes for comparison to the basis set. These mode shapes are quantified in terms of basis vector components that are expressed concisely in matrix form. Visual comparisons of the mode shapes to the basis vectors show that the numeric characterizations are consistent with the visual interpretations. Comparison of the four configurations to one another indicates that the numeric components distinguish subtle differences in wing deformation as well as differences in the overall shape of the deformed wing.

## Nomenclature

$B$	=	matrix of basis vectors
$\mathbf{b}^j$	=	the $j$ th basis vector
$I$	=	identity matrix
$K$	=	system stiffness matrix
$M$	=	system mass matrix
$n$	=	number of degrees of freedom of the structural model
$P$	=	projection matrix
$Q$	=	matrix of structural eigenvectors
$\mathbf{q}^i$	=	the $i$ th structural eigenvector
$s$	=	number of eigenvectors in reduced set for structural model
$t$	=	number of eigenvectors in reduced set for reference structural model
$\mathbf{x}$	=	system coordinate for structural model
$\Phi$	=	modal matrix
$\Phi^*$	=	matrix of reduced set of normal modes

## Introduction

THE examination of mode shapes is fundamental to the prediction of aircraft aeroelastic phenomenon such as flutter. Evaluation of the normal modes of the aircraft structure, or the flutter modes themselves, provides insight into the effects of wing deformation shape on aeroelastic behavior. Mode shapes derived from linear flutter analysis are used to study wing deformations associated with nonlinear aeroelastic oscillations and to assess the aeroelastic sensitivity of these deformations. This assessment is made by identifying the modes most likely to extract energy from the airstream, and the results are combined with flutter analysis instability results to predict linear and nonlinear aeroelastic behavior. In some cases, linear flutter analysis mode shapes are used to predict nonlinear aeroelastic behavior by correlating the modes to flight test results [1].

Received 18 Feb. 2009; revision received 7 Aug. 2009; accepted for publication 11 Aug. 2009. Copyright © 2009 by the American Institute of Aeronautics and Astronautics, Inc. The U.S. Government has a royalty-free license to exercise all rights under the copyright claimed herein for Governmental purposes. All other rights are reserved by the copyright owner. Copies of this paper may be made for personal or internal use, on condition that the copier pay the \$10.00 per-copy fee to the Copyright Clearance Center, Inc., 222 Rosewood Drive, Danvers, MA 01923; include the code 0021-8669/09 and \$10.00 in correspondence with the CCC.

\*Senior Flutter Engineer, U. S. Air Force SEEK EAGLE Office, 205 West D Avenue, Suite 348, Member AIAA.

Historically, mode shape evaluation for flutter prediction has been a qualitative process using visual images of aircraft node lines or modal deflections. Mode shapes of one aircraft configuration are visually compared with the shapes of a configuration with known flight test results, and these comparisons relate the mode shapes to nonlinear aeroelastic responses. The wing shapes are often described in terms of their similarity to a set of known reference shapes derived from a baseline wing design or configuration. This permits the description of arbitrary wing shapes in terms of identifiable physical shapes.

Although effective, these visual comparisons are subjective and do not provide quantitative descriptions of mode shapes. A quantitative approach using numeric descriptions of mode shapes offers an objective means to compare wing modes and to relate them to a set of reference wing shapes. The precision of a numeric description can also distinguish important shape differences and provide numerical data that are well suited for alternative aeroelastic prediction algorithms [2]. An obvious quantitative description scheme is to use the deformation values of points on the wing as the numeric descriptors. For a finite element wing model, the points could correspond to the grid points of the finite element mesh. However, the numeric descriptor for a single wing shape would consist of numerous deformation values according to the number of wing points used. In many cases, this would result in a cumbersome descriptor that would be difficult to use in comparison studies. The large number of numeric values for one mode shape would complicate the ability to categorize shapes, and the comparison of shapes with reference wing shapes would be tedious.

Therefore, the ability to concisely identify a mode shape requires a descriptor that relates the mode shape to each reference shape with a single number. In this approach, the number of descriptors equals the number of reference wing shapes used, and this permits further simplification when the reference shapes can be reduced to the smallest number possible. Selection of this reduced set of wing shapes can be accomplished by determining which shapes are needed to adequately model the aeroelastic mechanisms. This reduction of the reference set facilitates the concise identification of mode shapes in terms of a small number of physical shapes (such as wing bending, torsion, etc.).

In addition to offering concise description of mode shapes in terms of physical shapes, a numeric descriptor provides the precision and resolution necessary to describe subtle shape differences that are important to flutter prediction. Small, local shape effects such as minor changes in deformed wingtip orientation and node line position provide significant insight into flutter behavior. The evaluation

of these local shape effects can be improved by using a numeric descriptor that offers the precision and resolution necessary to distinguish subtle shape differences. In addition, the precision of a numeric descriptor provides the ability to quantify shape effects in numeric procedures such as neural network algorithms used for aeroelastic prediction. These networks estimate aeroelastic response based on a training routine that calibrates predictive models to flight test results, and numerically quantified mode shapes can be used as input parameters for these routines.

The use of numeric mode shape parameters in neural networks has been studied by Denegri and Johnson [2]. Their approach used four selected analytical mode shapes distinguished qualitatively by their node lines, and the four mode shapes were arbitrarily assigned integer values to provide the network with numeric shape data. Although this technique provides a numeric descriptor based on reference shapes, the use of integers limits the ability to describe shapes that are different from the four original shapes. Mode shapes that do not align closely with one of the original shapes may not be well described due to the lack of resolution of an integer quantifier.

A mode shape descriptor that is not limited to integer values was developed by Maxwell and Dawson [3]. Their technique incorporates a mode shape descriptor that uses the wingtip launcher motion to describe the wing motion of a fighter aircraft. This method quantifies the launcher's position and angle by determining the horizontal motion of the intersection point between the deflected launcher and the launcher equilibrium position. The technique includes parameters that describe phase differences between the launcher pitching and vertical motions. For structural normal modes, this phase difference is zero. However, the phase difference may not be zero for flutter mode shapes, and the method addresses phase relationships that influence the wing's interaction with the airstream. In contrast to the integer quantifier described above, this method provides the numeric resolution needed to specify the launcher position and phasing. However, there is no numeric description of the wing shape inboard of the launcher, and, therefore, the full wing shape is not described. In addition, this technique does not concisely compare shapes to a set of reference shapes.

Another method that has been studied by Denegri uses polynomial curve fits of the forward and aft wing spar deflections to define the wing mode shapes [4]. These curve fits produce polynomial coefficients that can be used as shape descriptors, and plots of the coefficient values are used to compare mode shapes. Although this method captures some of the wing shape inboard of the wingtip, it does not describe the full wing shape or the wingtip motion extensively. It is possible that a 2-D polynomial fit could be applied to capture the shape of the full wing surface. However, the large number of polynomial coefficients required may not produce a concise descriptor that facilitates comparison of the modes to reference shapes. In addition, curve fit methods approximate wing shapes, and, therefore, these techniques may not adequately depict small changes in the wing shapes.

Suciu and Buck reported a method using strain energy values computed at various locations of the aircraft structural model to identify and name the mode shapes [5]. Mode shapes are identified by relating the magnitude and location of strain energy values to various types of aircraft deformation. The naming of the mode shapes is automated by a computer algorithm that relates modal character to the aircraft structure's strain energy distribution. This approach offers an effective way to identify and name global mode shapes; however, it is not designed to distinguish subtle changes to wing shape. In addition, the use of energy values could produce nonunique descriptors that do not distinguish some shape features needed for flutter prediction methodologies.

To address the need for a unique numeric descriptor that describes mode shapes in terms of identifiable physical shapes, the method presented in this paper uses orthonormal basis vectors. The structural modes of an arbitrary wing are related numerically to basis vector shapes generated from a reference wing model, providing a known set of reference shapes by which mode shapes are concisely identified.

## Methodology

The orthonormal basis vectors used to describe wing modes are numeric representations of a set of reference wing shapes that are used as a baseline for describing other wing shapes. These reference wing shapes are produced from the normal mode eigenvectors of a reference wing model that is the primary structural model of the wing. Wing models that differ from the reference wing, such as those representing wings with structural enhancements or store attachments, are quantified in terms of the basis vectors. These alternate wing configurations are numerically identified by projecting their mode shapes onto the basis vectors using dot product multiplication. This is analogous to defining a 2-D arrow vector by its scalar projections onto the  $x$  and  $y$  axes. The resulting projection values represent the mode shape's component on each basis vector, and these components are used as the numeric descriptor. This provides a concise descriptor that relates each mode shape to each basis vector using a single number.

The normal mode eigenvectors from the reference wing model are orthogonalized and normalized to create the basis vectors. The resulting orthonormal basis provides a consistent numeric descriptor that is based on a 0–1 scale. Because two or three structural modes typically dominate flutter motions, only the normal mode eigenvectors that primarily participate in the flutter mechanism are used. This further simplifies the descriptor by reducing the number of basis vectors to a smaller set.

The vector projection concept has been previously applied to structural mode shapes for various test and analysis techniques. Desforges et al. used the modal assurance criterion to compare flutter flight test shapes between test points at successive airspeeds [6]. Although this technique does not directly quantify response shapes in terms of vector projections, the modal assurance criterion provides comparisons of mode shapes using a number derived from projection values. In addition, Przekop and Rizzi have used structural modes to provide an efficient modal basis for order reduction of nonlinear finite element simulations [7]. Their technique expresses the equations of motion in coordinates obtained by selecting a reduced set of structural basis vectors.

## Theoretical Development

The normal mode eigenvectors used to create the basis vectors are generated from the structural dynamic analysis of the reference wing or aircraft model. The structure is typically modeled as an autonomous conservative system with  $n$  degrees of freedom:

$$M\ddot{\mathbf{x}} + K\mathbf{x} = \mathbf{0} \quad (1)$$

Solution of the resulting eigenvalue problem yields the  $n \times n$  modal matrix  $\Phi$  for which the columns are the eigenvectors of Eq. (1). If the system contains only static coupling, the mass matrix is a diagonal matrix and, therefore, symmetric.

The basis vectors are created from the normal mode eigenvectors for the system described in Eq. (1). To create a concise set of basis vectors, a subset of the eigenvectors in  $\Phi$  is selected. Although the selection of the subset of eigenvectors can be arbitrary, the eigenvectors selected from  $\Phi$  should provide the mode shapes that are relevant to the flutter analysis. If this selected set is represented as  $\Phi^*$ , the size of  $\Phi^*$  is  $n \times t$  with  $t < n$ .

The need to orthogonalize the eigenvectors derives from their orthogonality properties from normal mode theory. According to the theory

$$\Phi^T M \Phi = I \quad (2)$$

due to the symmetry of the mass matrix  $M$ . Because, in general,  $M$  does not have equal diagonal elements:

$$\Phi^T \Phi \neq I \quad (3)$$

Because  $\Phi^*$  is a subset of  $\Phi$ , it is apparent from Eq. (2) and (3) that the columns of  $\Phi^*$  are orthogonal with respect to the system mass matrix but not to each other. To create a set of basis vectors that can distinguish modal characteristics adequately, an orthogonal set of

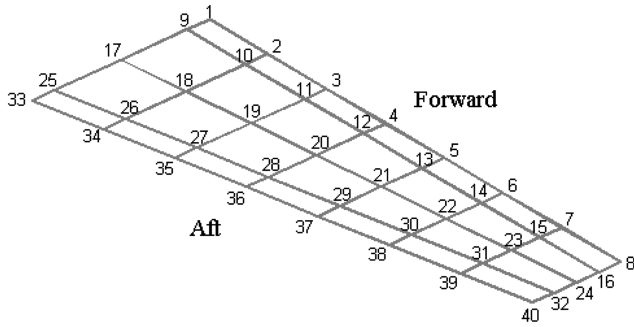


**Fig. 1 Wing model.**

basis vectors is generated by orthogonalizing the columns of  $\Phi^*$  using the Gram–Schmidt procedure. The Euclidean norms (vector magnitudes) of these orthogonalized vectors are set to a value of 1, and the resulting basis vectors  $\mathbf{b}^j$  are expressed as columns of the  $n \times t$  matrix  $B$ . Because of the orthogonalization and normalization

$$B^T B = I \quad (4)$$

Once the basis vectors are defined using a reference structural model, mode shapes from a different structural model can be quantified by comparing them to the basis vectors. Although all of the eigenvectors can be quantified, a subset of eigenvectors that is relevant to flutter analysis would typically be chosen for study. The reduced set of modal eigenvectors is then normalized by setting the Euclidean norms of the vectors to one. If  $n$  represents the number of eigenvectors produced by the model to be studied and  $s$  is the number of eigenvectors  $\mathbf{q}^i$  in the reduced set, then the modal eigenvectors can be represented by the  $n \times s$  matrix  $Q$  for which the columns are the  $\mathbf{q}^i$  with  $s < n$ . The eigenvectors are then quantified by comparison to the basis set by

$$P = Q^T B \quad (5)$$

The  $s \times t$  matrix  $P$  contains elements that are the scalar projection values between the normal mode eigenvectors and the basis vectors.

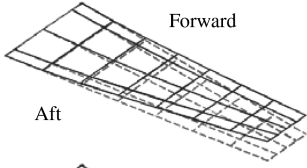
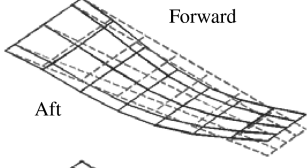
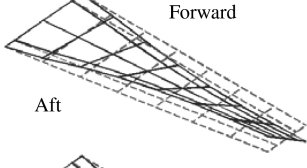
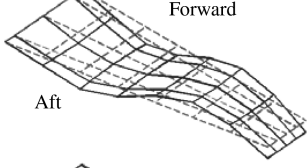
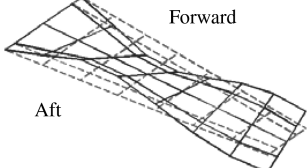
Because the eigenvectors in  $Q$  and the basis vectors in  $B$  are normalized to a Euclidean norm of 1, the comparison between the  $\mathbf{q}^i$  and the  $\mathbf{b}^j$  is based on projection values in  $P$  ranging from 0–1. Determination of the correspondence of a particular mode shape to the basis vectors is made by inspecting the projection values and their relative position on the 0–1 scale. A projection value of 1 indicates a normal mode eigenvector that is exactly the same shape as the basis vector being used for the comparison. A projection value of 0 indicates a normal mode eigenvector that is orthogonal to the basis vector being used. Thus, the proximity of the values in  $P$  to zero or one provides quantification of the normal mode shapes in terms of each shape in the basis set.

Because of the fact that the dot product operation sums the products of corresponding grid points, the grid point distribution becomes a consideration when wing models have a higher

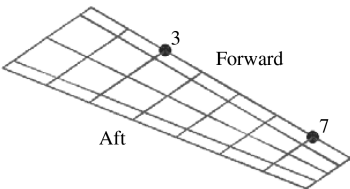
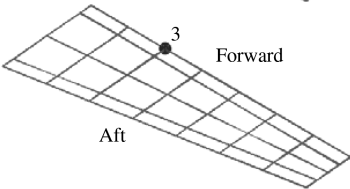
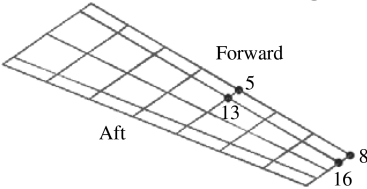
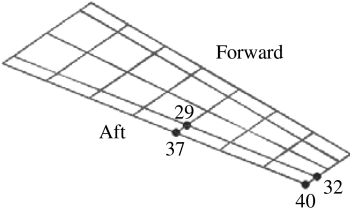
**Table 1 Wing model parameters**

Wing semispan, in.	144.25
Root chord, in.	54.06
Taper ratio	0.5
Sweep, deg	0.0
Dihedral, deg	0.0
Twist, deg	0.0
Shell thickness, in.	1.00 tapered to 0.00 at leading and trailing edges
Shell density (lb/in. <sup>3</sup> )	0.098
Shell elastic modulus, psi	$9.2418 \times 10^6$
Shell shear modulus, psi	$3.4993 \times 10^6$

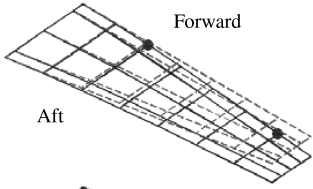
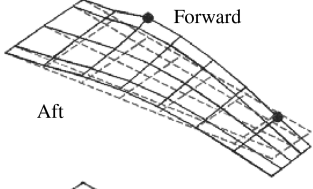
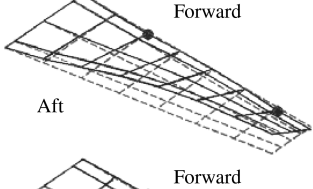
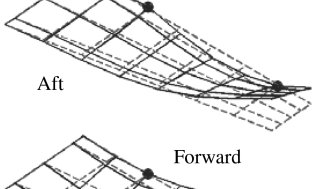
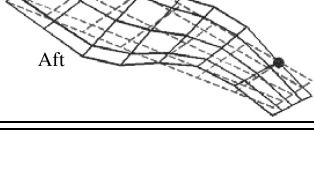
**Table 2 Basis vectors**

Basis vector shape	Description	Abbreviation
	First wing bending	1WB
	Second wing bending	2WB
	First wing torsion	1WT
	Third wing bending	3WB
	Second wing torsion	2WT

**Table 3 Wing configuration parameters**

Configuration	Visual depiction of concentrated mass locations	Concentrated mass value, lb
Two heavy forward		500.0
One heavy forward		500.0
Light forward		50.0
Light aft		50.0

**Table 4 Two heavy masses forward modal vectors**

Mode number	Modal eigenvector shape	Frequency, Hz	Visual description	Basis vector components
1		0.7	First wing bending	First wing bending
2		4.4	Second wing bending	Second wing bending
3		7.9	First wing bending, first wing torsion	First wing bending, first wing torsion
4		14.4	Second wing bending	First wing bending, second wing bending
5		26.7	Third wing bending, second wing torsion	Third wing bending, second wing torsion

$$P = \begin{matrix} & \begin{matrix} \text{1WB} & \text{2WB} & \text{1WT} & \text{3WB} & \text{2WT} \end{matrix} \\ \begin{bmatrix} -1.0 & 0.0 & 0.0 & 0.0 & 0.0 \\ -0.2 & -0.9 & -0.2 & -0.1 & -0.1 \\ 0.7 & -0.3 & 0.6 & 0.0 & 0.0 \\ 0.5 & 0.7 & 0.3 & -0.2 & -0.2 \\ 0.0 & -0.2 & -0.3 & 0.8 & -0.5 \end{bmatrix} & \begin{matrix} 1 \\ 2 \\ 3 \\ 4 \\ 5 \end{matrix} \end{matrix} \begin{matrix} \\ M \\ O \\ D \\ E \end{matrix}$$

Fig. 2 Projection matrix for two heavy masses forward configuration.

concentration of points in one area than in another area of the wing. A wing area with higher grid point density will be weighted more heavily in the shape comparison than those areas with lower grid point density. Thus, for wing models with a significantly nonuniform grid point distribution, a weighting correction to Eq. (5) based on the density of each grid point should be considered.

The relevance of the structural normal modes, and, therefore, the basis vectors, to flutter analysis is rooted in their role as contributors to the flutter eigenvectors. This contribution is based in the fact that the flutter eigenvectors may be composed of all normal modes  $\mathbf{q}^i$ . Because the size reduction of the basis vector set means there will be fewer basis vectors than the original number of eigenvectors in the model, the basis vectors do not contain the complete structural or flutter mode shape information. More rigorously, the basis vectors span a subspace of the vector space spanned by the normal mode and flutter mode eigenvectors. Thus, appropriate selection of normal mode eigenvectors is required so that the basis vectors adequately describe the flutter mechanism. This is accomplished by using the fact that flutter motion is generated by the coalescence of two or more flutter modes. These modes are typically dominated by two to three structural modes for which the frequencies closely correspond to the flutter frequencies, and these usually consist of the lower frequency

wing bending and torsion modes. Therefore, the choice of the modal vectors in  $\Phi^*$  from the vectors in  $\Phi$  is based on selection of the normal mode shapes that are significant descriptors of the flutter eigenvectors.

### Application to Wing Model

The procedure is demonstrated on the simple tapered wing shown in Fig. 1. The wing is a single layer model constructed of 40 grid points to which shell elements with nonzero densities are attached. No concentrated mass elements are attached to this version of the wing model, and it is used as the reference wing for generation of the basis vectors. The wing model parameters are summarized in Table 1.

#### Basis Vector Development

A modal analysis was performed on the reference wing model, and the resulting eigenvectors were orthogonalized to produce the basis vectors. Table 2 shows the shapes represented by the reduced set of basis vectors  $\mathbf{b}^j$ . As shown in Table 2, the wing configuration produces pure wing bending and torsion modes. The vectors beyond basis vector 5 are not included because they represent complicated mode shapes that are not typically relevant to flutter analysis. Because the significant contribution to the deflection shape is provided by the vertical displacements, the computation of the basis vectors and subsequent computations in this example only use the vertical deformations to define the shape.

#### Modified Wing Configurations

To provide alternate wing configurations for which the mode shapes can be quantified by the reference wing basis vectors, concentrated mass elements were added to simulate variations in wing mass. The addition of the concentrated mass elements at several locations resulted in four alternate wing versions that produce various

Table 5 One heavy mass forward modal vectors

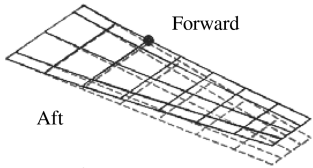
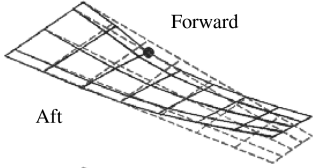
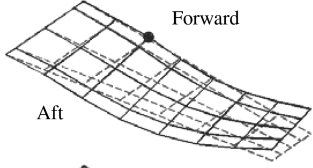
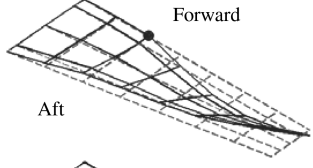
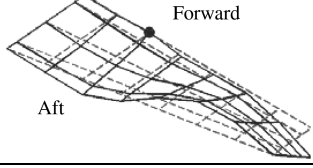
Mode number	Modal eigenvector shape	Frequency, Hz	Visual description	Basis vector components
1		1.5	First wing bending	First wing bending
2		4.7	Second wing bending	First wing bending, second wing bending
3		11.1	Second wing bending, first wing torsion	Second wing bending, first wing torsion
4		20.0	First wing torsion, third wing bending	First wing torsion, third wing bending
5		29.5	Third wing bending, second wing torsion	First wing torsion, third wing bending, second wing torsion

Table 6 Light masses forward modal vectors

Mode number	Modal eigenvector shape	Frequency, Hz	Visual description	Basis vector components
1	Forward	1.1	First wing bending	First wing bending
	Aft			
2	Forward	5.7	Second wing bending	Second wing bending
	Aft			
3	Forward	10.9	First wing torsion	First wing bending, first wing torsion
	Aft			
4	Forward	19.5	Third wing bending	Third wing bending
	Aft			
5	Forward	31.7	Second wing torsion	Third wing bending, second wing torsion
	Aft			

types of mode shapes. These configurations are summarized in Table 3. They consist of two heavy configurations with 500 lb. masses added to one or two leading edge locations and two light configurations with 50 lb. masses added to four leading or trailing edge locations. Modal analyses were performed for the four modified wing models in Table 3, and the eigenvectors  $\mathbf{q}'$  for these configurations were quantified by their projections onto the basis vectors. Because of the relative uniformity of the grid point distribution, no grid point density weighting was used in the projection matrix computations.

BASIS VECTOR

1WB

2WB

1WT

3WB

2WT

$$P = \begin{bmatrix} 1.0 & 0.0 & 0.0 & 0.0 & 0.0 \\ 0.8 & 0.6 & 0.3 & 0.1 & 0.1 \\ 0.2 & 0.8 & -0.5 & -0.1 & -0.1 \\ 0.1 & 0.3 & 0.9 & -0.4 & -0.2 \\ -0.2 & -0.2 & 0.5 & 0.7 & -0.5 \end{bmatrix}$$

1

2

3

4

5

M

O

D

E

Fig. 3 Projection matrix for one heavy mass forward configuration.

BASIS VECTOR

1WB

2WB

1WT

3WB

2WT

$$P = \begin{bmatrix} 1.0 & 0.0 & 0.0 & 0.0 & 0.0 \\ 0.1 & -1.0 & 0.0 & 0.1 & 0.0 \\ -0.4 & 0.1 & -0.9 & 0.0 & 0.0 \\ 0.2 & 0.3 & 0.0 & 0.9 & -0.2 \\ 0.2 & 0.3 & 0.0 & -0.4 & -0.8 \end{bmatrix}$$

1

2

3

4

5

M

O

D

E

Fig. 4 Projection matrix for light masses forward configuration.

Two Heavy Masses Forward Configuration

The shapes of the modal eigenvectors for the configuration with two heavy masses located on the forward edge of the wing are shown in Table 4. Table 4 also shows the associated modal frequencies, the visual descriptions of the mode shapes, and the description of the mode shapes based on their numeric basis vector components.

The visual descriptions in Table 4 are names given to the mode shapes as determined by qualitative visual interpretation of the shapes shown in the modal eigenvector shape plots. The naming of the shapes is based on descriptions traditionally used in flutter analysis. The shapes are described in visual terms by designating the most significant aspects of their bending or twisting character as determined by visual comparisons to the basis vectors in Table 2. The basis vector components in Table 4 are names given to the mode shapes as determined by their numeric descriptors, which are shown in the projection matrix  $P$  in Fig. 2. The numeric descriptors are the mode shapes' projection values onto the basis vectors, and, therefore, the basis vector components designate the numeric similarity of the mode shapes to the basis vector shapes.

The rows of  $P$  in Fig. 2 correspond to the mode shape number, and the columns of  $P$  correspond to the basis vector number, as

BASIS VECTOR

1WB

2WB

1WT

3WB

2WT

$$P = \begin{bmatrix} -1.0 & 0.0 & 0.0 & 0.0 & 0.0 \\ 0.1 & -1.0 & 0.0 & 0.1 & 0.0 \\ -0.4 & 0.1 & 0.9 & 0.0 & 0.0 \\ -0.2 & -0.3 & 0.0 & -0.9 & -0.2 \\ -0.2 & -0.3 & 0.0 & 0.4 & -0.8 \end{bmatrix}$$

1

2

3

4

5

M

O

D

E

Fig. 5 Projection matrix for light masses aft configuration.

determined by the multiplication performed in Eq. (5). In Table 4, the most significant basis vector components are shown by including only the mode shapes possessing a projection value with an absolute value of 0.4–1.0.

To examine the consistency of the numerical technique with traditional visual methods, qualitative comparisons between the visual descriptions and the numerical results can be made. The visual description of the mode shapes in Table 4 indicates that mode 2 has significant second wing bending content with some minor torsion content. Inspection of the projection matrix in Fig. 2 shows that the numerical technique provides results that correspond to these interpretations. The significant second wing bending content in mode 2 is evidenced by the projection matrix element (2,2) value of  $-0.9$ , and the projection matrix element (2,3) value of  $-0.2$  represents the small first wing torsion component. Similar comparisons can be made to mode 3, which visually appears to have significant first wing torsion content with some first wing bending content. This is verified by the projection matrix values, which indicate a first wing torsion value of 0.6, a first wing bending value of 0.7, and a second wing bending value of  $-0.3$ . Table 4 also shows that the numeric descriptor reveals some first wing bending content in mode 4 that was not clearly evident from the visual description.

#### One Heavy Mass Forward Configuration

Whereas the preceding example indicates that the numeric projection values effectively describe the general visual shapes in terms of the basis vector shapes, comparison between the previous example and the configuration with one heavy mass forward indicates that the numeric descriptor can also distinguish substantial differences in mode shapes. The one heavy mass case, shown in Table 5, has third and fourth mode shapes that are visually different from the corresponding modes in the two heavy masses case. Upon

visual examination of mode 3 for both configurations, the wingtip for the one heavy mass case does not intersect the equilibrium position, whereas the wing with two heavy masses does. This appears to be caused by the wing with one heavy mass having more second wing bending content than the two heavy mass case. This is consistent with the projection values, which indicate a second wing bending value of  $-0.3$  for the two heavy mass case Fig. 2 and 0.8 for the one heavy mass wing Fig. 3. Visual comparison of the fourth mode indicates that the two heavy mass wing has less torsion content than the one heavy mass case, and this is captured numerically with first wing torsion values of 0.3 and 0.9 for the two and one heavy mass cases, respectively. The numeric descriptors for mode 2 and mode 5 for the one heavy mass case also reveal shape content that was not evident in the visual interpretations.

#### Light Masses Forward Configuration

In addition to comparisons that illustrate significant differences in mode shapes, comparison of the previous configuration with two heavy masses to the configuration with the forward light masses (shown in Table 6) is made to verify the numeric descriptor's ability to distinguish subtle shape differences. The third modes for these configurations reveal differences that are evident at the wingtip area. Minor differences in the node line location are exhibited by the slight change in the wingtip node point axial location for mode 3. This distinction is captured by the differences between projection values onto the first wing bending, second wing bending, and first wing torsion basis vectors as shown in Figs. 2 and 4.

Note that the difference referred to for mode 3 shapes is between the chordal location of the node point, or center of twist, for the wingtip. The difference referred to is not the opposite directions of the wing twist, which is quantified by the differences in sign of the bending and torsion projection values. The fact that all bending and

**Table 7 Light masses aft modal vectors**

Mode number	Modal eigenvector shape	Frequency, Hz	Visual description	Basis vector components
1	Forward	1.1	First wing bending	First wing bending
	Aft			
2	Forward	5.7	Second wing bending	Second wing bending
	Aft			
3	Forward	10.9	First wing torsion	First wing bending, first wing torsion
	Aft			
4	Forward	19.5	Third wing bending	Third wing bending
	Aft			
5	Forward	31.7	Second wing torsion	Third wing bending, second wing torsion
	Aft			

torsion projection values for mode 3 differ by a sign change between the configurations indicates that the mode shapes were simply generated in opposite deformation directions.

Similar small differences in shape can be seen in the second modes as signified by the slight torsion effect of the wing with two heavy masses that is not evident for the wing with the forward light masses. This minor visual difference is distinguished by the projection values for these configurations, which are slightly different for the first and second torsion modes. The two heavy masses configuration has first and second torsion mode projection values of  $-0.2$  and  $-0.1$ , respectively, whereas these values for the forward light masses configuration are both  $0.0$ .

#### *Light Masses Aft Configuration*

The next comparison is made between the previous configuration with light masses on the forward part of the wing to the configuration with light masses on the aft part of the wing. This comparison contrasts wing deformations that are mirror images of one another about the midchord line. Tables 6 and 7 indicate that these mass locations result in the same frequencies between the two configurations because the wing is symmetric with respect to the midchord line. However, the 3rd mode shapes are dissimilar with regard to the relative directions of the torsion and bending modes. That is, whereas each mode has negative bending shapes, the wing torsion directions are opposite. The opposite torsion directions result in third mode shapes with a forward skewed node line for the light masses forward case and an aft skewed node line for the light masses aft case. Inspection of the projection matrix values for mode 3 for both configurations Figs. 4 and 5 reveals first and second wing bending values that are of the same sign between the configurations and a first wing torsion value that is opposite in sign between the configurations. The absolute values of these projections are the same due to the symmetry of the system.

### Conclusions

The projection of modal eigenvectors onto a set of basis vectors provides a numeric descriptor that is well suited to the interpretation of flutter analysis mode shapes. The technique uses a reduced set of basis vectors derived from a reference wing model to generate concise numeric mode shape descriptors. The direct comparison of the mode shapes to these basis vectors facilitates mode shape identification in terms of physical wing shapes. Both the mode shape vectors and the basis vectors are composed of deformation values of points distributed over the entire wing surface. Therefore, the method provides sufficient numerical resolution to describe subtle shape features while addressing the overall shape of the wing.

The basis vector description of the mode shapes of a simple tapered wing model indicates that the projection values correlate to

the visual interpretation of the mode shapes. The comparisons show that the numerical technique is consistent with qualitative results and that the precision of the descriptor reveals shape information that is not apparent from visual examination. The ability of the numeric descriptors to distinguish small changes in shape is evidenced by the differences in the projection values for minor changes of the wingtip node line locations. Because the basis vector components correlate to shape features that include wingtip motions as well as global wing motions, the descriptor is capable of characterizing the full wing shape. In addition, mode shape comparisons indicate that the numeric descriptor's magnitude and sign distinguish shapes with forward and aft skewed node lines.

The capacity of the method to facilitate engineering analysis of the mode shapes is evidenced by the concise form of the projection matrix. For the case examined here, this conciseness derives from the ability to describe the wing model's flutter relevant mode shapes using only five basis vectors. In addition, the correlation of the visual comparisons to the numeric descriptions demonstrates that the method provides straightforward association of the numeric descriptor with physical wing shapes. In the cases analyzed here, proper selection of the configuration for the wing reference model provided easily identifiable bending and torsion shapes.

### References

- [1] Denegri, C. M. Jr., and Cutchins, M. A., "Evaluation of Classical Flutter Analyses for the Prediction of Limit Cycle Oscillations," AIAA Paper 97-1021, April 1997.
- [2] Denegri, C. M. Jr., and Johnson, M. R., "Limit Cycle Oscillation Prediction Using Artificial Neural Networks," *Journal of Guidance, Control, and Dynamics*, Vol. 24, No. 5, 2001, pp. 887–895. doi:10.2514/2.4824
- [3] Maxwell, D. L., and Dawson, K. S., "Analytical Aeroelastic Characteristics Of F-16 Asymmetric External Store Configurations," AIAA Paper 2004-1755, April 2004.
- [4] Denegri, C. M., "Simple Quantitative Method to Compare Aircraft Wing Mode Shapes," *Journal of Aircraft*, Vol. 46, No. 3, 2009, pp. 1082–1084. doi:10.2514/1.42777
- [5] Suci, E., and Buck, J., "Postprocessor for Automatic Mode Identification for MSC/NASTRAN Structural Dynamic Solutions with Emphasis on Aircraft Flutter Applications," *MSC/NASTRAN Americas Users' Conference*, Paper 1498, Los Angeles, Oct. 1998.
- [6] Desforges, M. J., Cooper, J. E., and Wright, J. R., "Mode Tracking During Flutter Testing Using the Modal Assurance Criterion," *Proceedings of the Institution of Mechanical Engineers*, Vol. 210, No 17, 1996, pp. 27–37. doi:10.1243/PIME\_PROC\_1996\_210\_342\_02
- [7] Przekop, A., and Rizzi, S. A., "Nonlinear Reduced-Order Analysis with Time-Varying Spatial Loading Distributions," AIAA Paper 2008-2323, April 2008.